

Clinical Cancer Research

Bendamustine (Treanda) Displays a Distinct Pattern of Cytotoxicity and Unique Mechanistic Features Compared with Other Alkylating Agents

Lorenzo M. Leoni, Brandi Bailey, Jack Reifert, et al.

Clin Cancer Res 2008;14:309-317. Published online January 2, 2008.

Updated Version Access the most recent version of this article at:
doi:[10.1158/1078-0432.CCR-07-1061](https://doi.org/10.1158/1078-0432.CCR-07-1061)

Cited Articles This article cites 39 articles, 15 of which you can access for free at:
<http://clincancerres.aacrjournals.org/content/14/1/309.full.html#ref-list-1>

Citing Articles This article has been cited by 14 HighWire-hosted articles. Access the articles at:
<http://clincancerres.aacrjournals.org/content/14/1/309.full.html#related-urls>

E-mail alerts [Sign up to receive free email-alerts](#) related to this article or journal.

Reprints and Subscriptions To order reprints of this article or to subscribe to the journal, contact the AACR Publications Department at pubs@aacr.org.

Permissions To request permission to re-use all or part of this article, contact the AACR Publications Department at permissions@aacr.org.

Bendamustine (Treanda) Displays a Distinct Pattern of Cytotoxicity and Unique Mechanistic Features Compared with Other Alkylating Agents

Lorenzo M. Leoni,^{1,2} Brandi Bailey,^{1,3} Jack Reifert,^{1,6} Heather H. Bendall,^{1,4} Robert W. Zeller,³ Jacques Corbeil,^{7,9} Gary Elliott,^{1,5} and Christina C. Niemeyer^{1,8}

Abstract Purpose: Bendamustine has shown clinical activity in patients with disease refractory to conventional alkylator chemotherapy. The purpose of this study was to characterize the mechanisms of action of bendamustine and to compare it with structurally related compounds. **Experimental Design:** Bendamustine was profiled in the National Cancer Institute *in vitro* antitumor screen. Microarray-based gene expression profiling, real-time PCR, immunoblot, cell cycle, and functional DNA damage repair analyses were used to characterize response to bendamustine and compare it with chlorambucil and phosphoramidate mustard. **Results:** Bendamustine displays a distinct pattern of activity unrelated to other DNA-alkylating agents. Its mechanisms of action include activation of DNA-damage stress response and apoptosis, inhibition of mitotic checkpoints, and induction of mitotic catastrophe. In addition, unlike other alkylators, bendamustine activates a base excision DNA repair pathway rather than an alkyltransferase DNA repair mechanism. **Conclusion:** These results suggest that bendamustine possesses mechanistic features that differentiate it from other alkylating agents and may contribute to its distinct clinical efficacy profile.

Bendamustine, 4-{5-[bis(2-chloroethyl)amino]-1-methyl-2-benzimidazolyl} butyric acid hydrochloride, also known as Treanda (Cephalon, Inc.) and marketed in Germany as Ribomustin (Mundi Pharma Ltd.), is a purine analogue/alkylator hybrid cytotoxic with shown clinical activity against various human cancers including non-Hodgkin's lymphoma (1, 2), chronic lymphocytic leukemia (3), multiple myeloma (4, 5), breast cancer (6), and small-cell lung cancer (7, 8). In addition, both preclinical (9–11) and clinical (12) studies of bendamustine have shown activity in cancer cells that are resistant to conventional alkylating agents.

Bendamustine was originally designed to have both alkylating and antimetabolite properties with acceptable toxicity (13). Structurally, bendamustine comprises three elements: a 2-chloroethylamine alkylating group, a benzimidazole ring,

and a butyric acid side chain (Fig. 1). The 2-chloroethylamine alkylating group is shared with other members of the nitrogen mustard family of alkylators, which includes cyclophosphamide, chlorambucil and melphalan, and the butyric acid side chain is shared with chlorambucil. The benzimidazole central ring system is unique to bendamustine; the intent of adding this structure to the nitrogen mustard was to include the antimetabolite properties shown for benzimidazole (14, 15). This heterocyclic ring structure may contribute to the unique antitumor activity of bendamustine and distinguish it from conventional 2-chloroethylamine alkylators (16).

Although a large body of clinical data on bendamustine in a variety of tumors has been reported, studies clearly defining the mechanisms of action of bendamustine are lacking. Similar to other alkylators, bendamustine is a DNA cross-linking agent that causes DNA breaks. However, DNA single- and double-strand breaks caused by bendamustine are more extensive and significantly more durable than those caused by cyclophosphamide, cisplatin, or carmustine (bischloroethyl nitrosourea; ref. 9). The DNA damage mediated by alkylators has been associated with a regulated form of necrotic cell death (17). Bendamustine as a single agent (18–20) or in combination with other anticancer agents (21) has also shown proapoptotic activity in several *in vitro* tumor models.

The objective of the current study was to describe potential mechanisms of action of bendamustine that distinguish it from other alkylators using large-scale screening technologies, including the National Cancer Institute (NCI) *In vitro* Cell Line Screening Project (IVCLSP) and gene microarrays. We report data from these analyses and confirm a unique antitumor activity profile for bendamustine compared with

Authors' Affiliations: ¹Salmexid, acquired by Cephalon, Inc., Frazer, Pennsylvania; ²Telormedix, Lugano, Switzerland; ³Department of Biology, San Diego State University; ⁴Neurocrine, Inc.; and ⁵Galenic Strategies, San Diego, California; ⁶University of California Santa Barbara, Santa Barbara, California; ⁷Center for AIDS Research, Center for Molecular Medicine and Cancer Center, University of California San Diego and ⁸Burnham Institute for Medical Research, La Jolla, California; and ⁹Quebec City Genome Centre, Laval University, Quebec, Canada

Received 5/3/07; revised 9/25/07; accepted 10/10/07.

The costs of publication of this article were defrayed in part by the payment of page charges. This article must therefore be hereby marked *advertisement* in accordance with 18 U.S.C. Section 1734 solely to indicate this fact.

Requests for reprints: Christina Niemeyer, Burnham Institute for Medical Research, 10901 North Torrey Pines Road, La Jolla, CA 92037. Phone: 858-646-3100; Fax: 858-795-5221; E-mail: niemeyer@burnham.org.

© 2008 American Association for Cancer Research.

doi:10.1158/1078-0432.CCR-07-1061

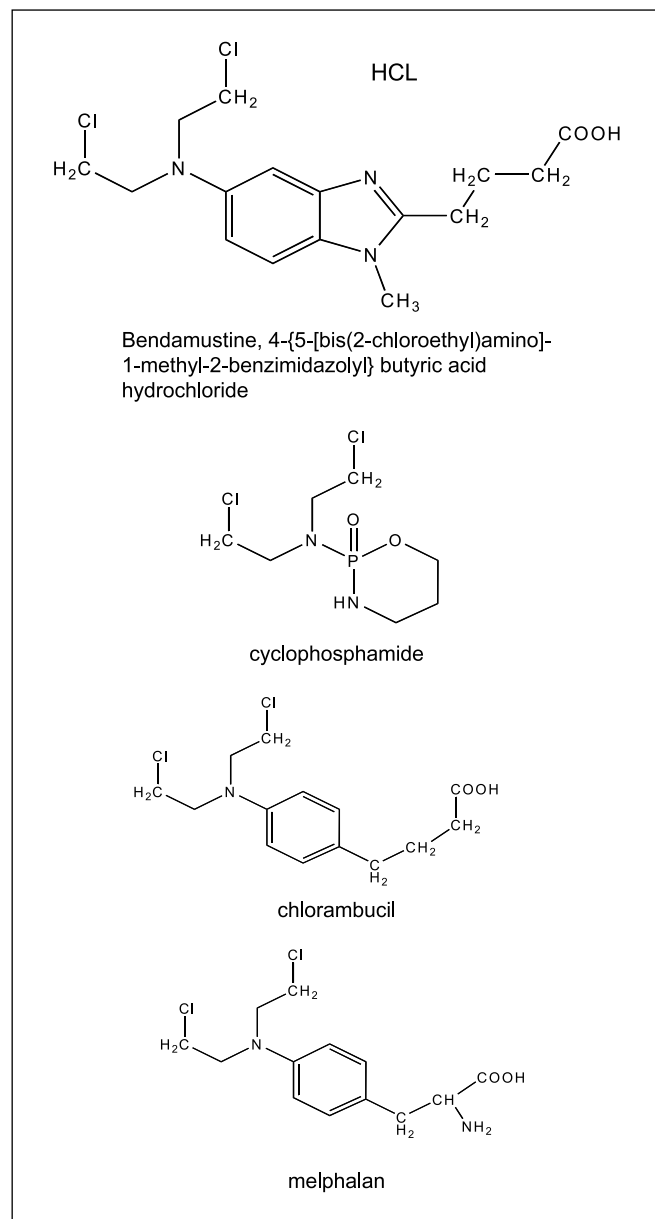


Fig. 1. Structures of bendamustine, cyclophosphamide, chlorambucil, and melphalan.

cyclophosphamide, chlorambucil, and melphalan. We also report that bendamustine specifically regulates, transcriptionally and posttranslationally, genes involved in apoptosis, DNA repair, and mitotic checkpoints.

Materials and Methods

NCI antitumor screen (IVCLSP). The IVCLSP of the NCI Developmental Therapeutics Program screens up to 3,000 compounds annually for potential anticancer activity.¹⁰ This program uses 60 human tumor cell lines representing leukemia, melanoma, and cancers of the lung, colon, brain, ovary, breast, prostate, and kidney. In a two-stage

screening process, compounds are tested for growth-inhibitory activity in all 60 cell lines at a single dose of 10 $\mu\text{mol/L}$, and compounds that achieve a threshold activity are retested in all 60 cell lines in a five-dose screen. Further details of the NCI cell screening protocols and reporting procedures have been described previously (22). The growth-inhibitory activity of a tested compound is expressed as $\log(\text{GI}_{50}, \text{TGI}, \text{or LC}_{50})$, where GI_{50} is the concentration required to inhibit tumor cell growth by 50%, TGI is the concentration causing total growth inhibition, and LC_{50} is the lethal concentration at which 50% of cells are killed. For each compound tested, 60 activity values (one for each cell line) make up the activity pattern, or fingerprint, of the compound.

COMPARE analysis. The development and application of the COMPARE algorithm for finding correlations among compounds tested in the IVCLSP have been previously described (23) and the program is freely available on the Developmental Therapeutics Program Web site.¹¹ A Pearson correlation coefficient (PCC) of >0.8 indicates $>65\%$ agreement in the sensitivity patterns of two compounds and a high likelihood of a common mechanism of action (24).

Cells and reagents. SU-DHL-1 and SU-DHL-9 cells were obtained from the University of California San Diego. Daudi, Raji, MCF-7/ADR, and RKO-E6 cells were obtained from American Type Culture Collection. Cells were grown in RPMI 1640 (Hyclone) supplemented with 10% fetal bovine serum (Invitrogen) and 100 units/mL penicillin/streptomycin.

Bendamustine hydrochloride was obtained from Astellas. Phosphoramidate mustard cyclohexylamine salt (NSC69945), an active metabolite of cyclophosphamide (25), was obtained from the synthetic repository of the Developmental Therapeutics Program. Each drug compound was prepared in DMSO and then diluted in culture medium. Inhibitory concentrations of 50% (IC_{50}) or 90% (IC_{90}) were determined by the 3-(4,5-dimethylthiazol-2-yl)-2,5-diphenyltetrazolium bromide (MTT) viability assay after 3 days of cell exposure to drug.

Preparation of RNA samples and microarray experiments. SU-DHL-1 cells were incubated with bendamustine at IC_{50} (25 $\mu\text{mol/L}$) and IC_{90} (35 $\mu\text{mol/L}$). Phosphoramidate mustard and chlorambucil were tested at IC_{90} of 50 and 5 $\mu\text{mol/L}$, respectively. These concentrations reflect clinically achievable plasma levels for each drug when administered at recommended doses (26). Gene expression was determined after 8 h of drug treatment to identify the proximal events related to drug exposure. Cells (5×10^6) were harvested in 1 mL TRIzol solution (Invitrogen) and total RNA was isolated as per manufacturer's instruction. Biotin-labeled cDNA (15 μg) was hybridized to each GeneChip array (Affymetrix). Briefly, the procedure to prepare material for hybridization to the chips involves multiple steps. Total RNA was isolated and quantified by absorbance. cDNA was generated using a specific primer that recognizes the polyadenylate tail coupled with a T7 promoter [dT7-(T)24] with deoxynucleotide triphosphate, DTT, and Superscript II to generate the first strand. This approach alleviates the need to isolate polyadenylate mRNA. The second strand was synthesized by adding deoxynucleotide triphosphate with DNA ligase, DNA polymerase I, and RNase H and incubating for 2 h at 16°C before adding T4 DNA polymerase for an additional 5 min. cDNA was column purified and quantified. *In vitro* transcription was done before hybridization to the high-density oligonucleotide arrays. The starting material for this reaction was 1 μg of cDNA to which nucleotide triphosphates were added with 25% less CTP and UTP to be compensated by adding 10 mmol/L biotinylated-11-CTP and 10 mmol/L biotinylated-16-UTP. The final addition of T7 enzyme in the appropriate buffer for 6 h at 37°C yielded the biotinylated *in vitro* transcription RNA that was then column purified (RNeasy, Qiagen). Chemically fragmented *in vitro* transcription RNA (15 μg) was mixed with control oligonucleotides, standards (including a housekeeping gene), and salmon sperm DNA in the appropriate buffer; heated to 95°C for 5 min; and hybridized to the chip for 16 h at 42°C.

¹⁰ <http://dtp.nci.nih.gov/branches/btb/ivclsp.html>

¹¹ <http://dtp.nci.nih.gov/>

Nonhybridized material was washed off with 2× saline-sodium phosphate-EDTA, and phycoerythrin-labeled avidin was then added to the chip. The excess fluorochrome was washed off and the chip was scanned for intensity of fluorescence in each synthesis feature (synthesis features are 7.5 μm²).

Bioinformatics analysis. The CORGON method was used to analyze scanned images of Affymetrix GeneChips (27). Only genes that showed a significant change in expression ($P < 0.05$) after bendamustine exposure when compared with untreated control cells were considered differentially regulated.

A Gene Ontology analysis (GO3 software) was used to elucidate molecular pathways selectively modulated by bendamustine compared with the other two drugs. The GO3 is an unbiased and unsupervised tool for finding statistically significant terms in the Gene Ontology database,¹² a controlled vocabulary developed to aid the description of the molecular functions of gene products and their participation in biological processes. Genes were chosen for clustering based on the similarity of their expression patterns using hierarchical clustering methods. This initial classification was used to determine the primary genes and pathways modulated by each test drug.

Quantitative PCR analysis. The *in vitro* expression levels of specific transcripts were determined using quantitative PCR (Q-PCR). Total RNA from each treated SU-DHL-1 cell pellet was isolated using an RNeasy mini-prep kit (Qiagen). cDNAs were made using a ThermoScript reverse-transcriptase kit (Invitrogen) and oligo-dT primers according to manufacturer's protocol. Q-PCR amplification and quantitation were carried out using an iCycler machine (Bio-Rad). Sample amplification was done in a volume of 25 μL containing 12.5 μL of 2 × IQ SybrGreen Mix (Bio-Rad), 1 μmol/L of each primer, and a volume of cDNA corresponding to 80 ng of total RNA. Cycling conditions were as follows: 95°C for 5 s, 30 s at the appropriate annealing temperature for each primer, and 72°C for 30 s. Target specificity of the assays was validated by melt curve analysis. The expression of each gene was normalized relative to 18S expression levels for each sample. The expression of each gene relative to untreated control was calculated using the 2^{-ΔΔC_t} method of Livak and Schmittgen (28). Primers were designed using Beacon Designer (Premier Biosoft) or designed based on the literature. Primer sequences and annealing temperatures are as follows: 18S, 5'-CGCCGCTAGAGGTGAAATTC-3', 5'-TTGGCAAATGCTTTTCGCT-3' (55°C); p21, 5'-CCTCATCCCCGTGTTCTCCTTT-3', 5'-GTACCACCCAGCGACAAGT-3' (57°C); NOXA, 5'-ATTTCTTCGGTCACTACACAA-3', 5'-AACGCCAACAGGAACAC-3' (55°C); PLK-1, 5'-CTCAACACGCCTCATCCT-3', 5'-GTGCTCGCTCATGTAATTGC-3' (57°C); Aurora A, 5'-TCCTGTGCAGATTCCATTACCTGT-3', 5'-GAATGCGCTGGGAAGAAATTTG-3' (55°C); Aurora B, 5'-AGAGTGATCACACAACGAGA-3', 5'-CTGAGCAGTTGGAGATGAGGTC-3' (56°C); cyclin B1, 5'-AGTGTGACCCAGACTGCCTC-3', 5'-CAAGCCAGGTCACCTCCTC-3' (57°C); Exo1, 5'-TTGGTCTGGAGGTCCTTGGAGA-3', 5'-GAATCGCTCTTCTTCGGAAGTGC-3' (57°C).

Western blot analysis. SU-DHL-1 cells were incubated with equitoxic (IC₅₀) concentrations of bendamustine (50 μmol/L), chlorambucil (2 μmol/L), or phosphoramidate mustard (20 μmol/L) for 20 h. Cells were washed twice with 1× PBS and lysed for 1 h with ice-cold lysis buffer [1 mol/L Tris-HCl (pH 7.4), 1 mol/L KCl, 5 mmol/L EDTA, 1% NP40, 0.5% sodium deoxycholate, with 1 mmol/L sodium orthovanadate, 1 mmol/L NaF, protease inhibitor cocktail (Roche), and phosphatase inhibitor cocktail (Sigma)] added directly before lysis. Nonsoluble membranes, DNA, and other precipitates were pelleted, and the protein supernatant was obtained. Protein concentrations were determined using the Bradford assay (Pierce). Twenty micrograms of lysate were separated by gel electrophoresis on a 4% to 12% polyacrylamide gel, transferred to nitrocellulose membranes (Invitrogen), and detected by immunoblotting using the following primary monoclonal antibodies: anti-p53, anti-phosphorylated p53 (Ser¹⁵-

specific), anti-p21, and anti-cleaved PARP (caspase-specific cleavage site; Cell Signaling); anti-Bax and anti-PARP (BD PharMingen); and anti-β-actin, used for a loading control (Sigma). Primary antibodies were incubated overnight at 4°C with gentle shaking. Membranes were washed thrice with 1× PBS and incubated with Alexa Fluor 680 goat anti-mouse secondary antibody (1:4,000; Molecular Probes) for 2 h at room temperature with gentle shaking. Blots were washed thrice with 1× PBS and scanned on a LiCor Odyssey scanner.

In vitro cell-based Ape-1 and alkylguanyl transferase assays. Cells were preincubated for 30 min with either 6 mmol/L methoxyamine (Sigma) or 50 μmol/L O⁶-benzylguanine (Sigma), inhibitors of Ape-1 base excision repair enzyme, or alkylguanyl transferase enzyme, respectively. The cells were then exposed to various concentrations of the test materials for 72 h. Cytotoxicity was evaluated by the MTT viability assay (29) and an IC₅₀ was determined as the drug concentration that inhibited by 50% the viability value of the untreated control. Analyses were done using GraphPad Prism version 3.00 GraphPad Software.

Cell cycle analyses. SU-DHL-1 cells were incubated with equitoxic (IC₅₀) concentrations of bendamustine (50 μmol/L), chlorambucil (4 μmol/L), or phosphoramidate mustard (50 μmol/L) for 8 h. Cells were washed with PBS and fixed in 70% ethanol at 20°C for at least 1 h. Fixed cells were rehydrated by washing with PBS. Cells were resuspended in a propidium iodide staining solution consisting of 10 μg/mL propidium iodide (Calbiochem), 10 μg/mL RNase A (DNase-free, Novagen), and 10 μL/mL Triton-X (Sigma) in PBS. Samples were analyzed using a FACSCalibur (BD Biosciences). Analyses of cell cycle distribution were done using DNA ModFit LT (Verity House Software, Inc.) modeling software.

Microscopy. MCF-7(ADR) or RKO-E6 cells were grown on slide microchambers and treated for 3 days with 25 μmol/L bendamustine. The slides were washed with PBS and mounted using SlowFade Light Antifade-DAPI mounting medium (Molecular Probes). Images were collected using a Zeiss Axioplan IIe epifluorescent microscope equipped with appropriate filters for 4',6'-diamidino-2-phenylindole imaging and Axiovision software (Carl Zeiss). Images were acquired with an Axiocam HrM using a C-apo ×40 Plan Neofluor objective. More than 500 cells were counted for each condition and all experiments were repeated at least thrice.

Results

Bendamustine displays a unique profile of activity using the NCI COMPARE analysis. The IVCLSP screen and COMPARE analysis were done for melphalan, chlorambucil, and the active metabolite of cyclophosphamide. Similar sensitivity patterns were shown for 25 compounds compared with melphalan (PCC >0.839), 25 compounds compared with chlorambucil (PCC >0.839), and 23 compounds compared with the active metabolite of cyclophosphamide (PCC >0.800). Agents that match most closely with these agents are all DNA-alkylating agents (Table 1A-C). Direct comparisons among cyclophosphamide, chlorambucil, and melphalan showed strong correlation coefficients (0.76-0.93).

In contrast, the sensitivity pattern of bendamustine did not strongly correlate with any of the compounds tested. In fact, of the top six matches (Table 1D), only dacarbazine showed a sensitivity agreement (r^2) exceeding 50%. The remaining matches for bendamustine included a topoisomerase 1 inhibitor, an anthracycline, and an antimetabolite, in addition to two other alkylators, including melphalan. These results suggest that bendamustine has a unique mechanistic profile compared with most conventional alkylators.

Microarray analysis of bendamustine, phosphoramidate mustard, and chlorambucil. To define the differences in molecular

¹² <http://www.geneontology.org/>

Table 1. Sensitivity patterns identified by COMPARE

Compound	NSC	Mechanism of action	Correlation (PCC), GI ₅₀
A. Melphalan			
Chlorambucil	3088	DNA alkylator, nitrogen mustard	0.934
Thio-TEPA	6396	DNA alkylator	0.909
Piperazine, 1-(2-chloroethyl)-4-(3-chloropropyl)-, dihydrochloride	344007	DNA alkylator, nitrogen mustard	0.913
2-Hexanamine, 1,6-dichloro- <i>N</i> -(2-chloroethyl)-, hydrochloride	9713	DNA alkylator, nitrogen mustard	0.902
YOSHI 864	102627	DNA alkylator	0.876
Hepsulfam	329680	DNA alkylator	0.875
B. Chlorambucil			
Uracil mustard	34462	DNA alkylator, nitrogen mustard	0.957
Aziridine, 1,1'-[tetramethyl- <i>p</i> -phenylenebis(methylenecarbonyl)]bis-Melphalan	48034	DNA alkylator	0.916
8806	8806	DNA alkylator, nitrogen mustard	0.896
Epoxy piperazine	74437	DNA alkylator	0.895
2-Hexanamine, 1,6-dichloro- <i>N</i> -(2-chloroethyl)-, hydrochloride	9713	DNA alkylator, nitrogen mustard	0.894
Diiodobenzotepa	167781	DNA alkylator	0.892
Piperazine, 1-(2-chloroethyl)-4-(3-chloropropyl)-, dihydrochloride	344007	DNA alkylator, nitrogen mustard	0.886
Vercyte	25154	DNA alkylator	0.880
Thio-TEPA	6396	DNA alkylator	0.875
C. Cyclophosphamide			
MX2 HCl	619003	Anthracycline, DNA intercalator	0.934
Fotrin	216135	DNA alkylator	0.878
1-Aziridinecarboxamide, <i>N,N'</i> -hexamethylenebis(2-methyl)	54059	DNA alkylator	0.877
Bis(2-chloroethyl)- <i>N</i> -methyl- <i>N</i> -(3-methyl-2-nitrobenzyl)ammonichloride	658929	DNA alkylator	0.852
Menogaril	269148	Anthracycline, DNA intercalator	0.847
Thio-TEPA	6396	DNA alkylator	0.832
YOSHI 864	102627	DNA alkylator	0.812
Melphalan	8806	DNA alkylator, Nitrogen mustard	0.765
Chlorambucil	3088	DNA alkylator, nitrogen mustard	0.762
D. Bendamustine			
CTIC, dacarbazine	45388	DNA alkylator, methylating agent	0.792 (LC ₅₀)
TOPT1B	376254	Topoisomerase I inhibitor	0.619 (TGI)
<i>N,N</i> -Dibenzyl-daunomycin	268242	Anthracycline, DNA intercalator (daunomycin analogue)	0.574 (TGI)
Melphalan	8806	DNA alkylator, nitrogen mustard	0.550 (GI ₅₀)
YOSHI 864	102627	DNA alkylator	0.542 (GI ₅₀)
Ara-AC (Fazarabine)	281272	Antimetabolite and DNA methylation inhibitor	0.524 (TGI)

NOTE: Twenty-five compounds showed a PCC of >0.839 for melphalan; 25 compounds showed a PCC of >0.839 for chlorambucil; 23 compounds showed a PCC of >0.8 for cyclophosphamide; and no compound showed a PCC of >0.8 for bendamustine.

mechanisms of action between bendamustine and conventional alkylators, we conducted gene expression analyses. Affymetrix GeneChip analysis was used to compare the expression levels of >12,000 genes in SU-DHL-1 cells, a non-Hodgkin's lymphoma cell line, after 8 h of treatment with bendamustine, phosphoramidate, chlorambucil, or no drug (see Materials and Methods for more details). Among the top 100 most modulated genes, most genes were up-regulated upon exposure to bendamustine, phosphoramidate, or chlorambucil, whereas only a subset was transcriptionally repressed.

The GO3 analysis comparing the DMSO-treated control and the bendamustine-treated SU-DHL-1 cells (at IC₉₀ dose) showed the highest statistical differences in the following major "functional groups": (a) response to DNA-damage stress; (b) DNA metabolism; (c) cell proliferation; and (d) cell regulation (Table 2). The profile obtained for phosphoramidate mustard showed significant changes in the biological processes,

including response to DNA damage or stress (GO6974), cell proliferation (GO8283), and regulation of biological process (GO50789) as well as cellular process (GO50794). A notable difference from bendamustine was the absence of several biological processes belonging to the "DNA metabolism, DNA repair, transcription" and "cell cycle, mitotic checkpoint" groups (Table 2).

The comparison between bendamustine and chlorambucil revealed even larger differences. Chlorambucil was only highly linked to two biological processes, regulation of biological process (GO50789) and regulation of cellular processes (GO50794; Table 2). The GO3 analysis was then used to compare the gene expression changes induced by bendamustine and chlorambucil side-by-side. Two main pathways were identified by this comparison as statistically different between the two compounds: nucleic acid metabolism and mitotic checkpoint-cell cycle regulation. The biological processes with

the highest *P* value in this side-by-side comparison were deoxyribonucleoside triphosphate metabolism (GO9200), deoxyribonucleotide metabolism (GO9262), and regulation of CDK activity (GO79).

Bendamustine uniquely regulates apoptosis pathways in non-Hodgkin's lymphoma cells compared with other alkylators. Many proapoptotic genes known to possess p53-response elements in their promoter regions, and considered to be p53-dependent, were found by the microarray analysis to be induced by bendamustine. p53 is an important tumor suppressor transcription factor that mediates apoptosis in response to DNA damage or other major cellular disruptions (30). Examples of these genes are *p21* (*Cip1/Waf1*/cyclin-dependent kinase inhibitor 1A; p53-induced cell division kinase inhibitor), *wip1* (p53-induced protein phosphatase 1), *NOXA* (p53-induced proapoptotic Bcl-2 family member), *DR5/KILLER* (p53-regulated DNA damage-inducible cell death receptor), and *BTG2* (p53-dependent component of DNA damage cellular response pathways). In addition to p53-related genes, other regulated genes related to apoptosis and identified in the top 100 modulated genes were four members of the tumor necrosis factor-receptor superfamily. Several of these genes have been shown to play a critical role in the regulation of the extrinsic apoptotic pathway (31).

Q-PCR validation was used to confirm the effects of bendamustine on *p21* (*Cip1/Waf1*) and *NOXA*. Both genes were induced in SU-DHL-1 cells after 8 h of exposure to bendamustine. Both genes were also induced by equitoxic concentrations of phosphoramidate mustard and chlorambucil, but to a much lower extent (Fig. 2A).

One of the key initial events known to trigger apoptosis through p53 is phosphorylation at Ser¹⁵ of p53. In an immu-

noblot analysis, using antibodies that specifically recognize Ser¹⁵-phosphorylated p53, bendamustine led to an 8-fold up-regulation of Ser¹⁵-phosphorylated p53 in SU-DHL-1 cells. In contrast, only minor up-regulation was seen in chlorambucil-treated cells, and no changes were observed in phosphoramidate mustard-treated cells at equitoxic concentrations (Fig. 2B).

A strong increase in the expression of total p53 was also seen in bendamustine-treated cells. Chlorambucil-treated cells showed a small increase in total p53, whereas phosphoramidate mustard induced no change in p53 levels (Fig. 2B) at equitoxic concentrations. Given the strong induction of p53 in bendamustine cells, we decided to test for potential changes in the proapoptotic mitochondrial protein, Bax. Although also a downstream effector of p53, due to a weaker p53-responsive element in its promoter, Bax has been reported to have a weaker induction than p21 in wild-type p53 cancer cells (32). Bendamustine, but not phosphoramidate or chlorambucil, caused an appreciable increase in the protein expression of Bax in SU-DHL-1 cells (Fig. 2B).

Bendamustine uniquely regulates DNA repair pathways in non-Hodgkin's lymphoma cells compared with other alkylators. Because DNA repair was characterized in the GO3 analysis as a "functional group" differentially regulated by bendamustine, several genes involved in DNA repair were analyzed by Q-PCR. One DNA repair gene that was found in the microarray to be induced was *exonuclease-1* (*EXO1*). Bendamustine induced a stronger (2.5-fold) up-regulation of *EXO1* expression compared with that observed with phosphoramidate mustard (1.5-fold) or chlorambucil (1.8-fold; Fig. 3A). Because DNA-repair capacity has been shown to play a critical role in resistance to DNA-alkylating drugs, these pathways may contribute to the different

Table 2. Gene Ontology consortium statistical analysis of bendamustine-induced gene changes in SU-DHL-1 cells

Functional groups	GO no.	GO description: biological process	BENDA	PM	CHLB
DNA-damage, stress response, apoptosis	6974	Response to DNA damage stress	0.00001	0.0041	NA
	6950	Response to stress	0.0003	NA	NA
	16265	Death	0.0482	NA	0.0428
DNA metabolism, DNA repair, transcription	6259	DNA metabolism	0.00003	0.0433	NA
	6139	Nucleobase, nucleoside, nucleotide, and nucleic acid metabolism	0.0004	NA	NA
	6357	Regulation of transcription from Pol II promoter	0.0003	NA	0.0109
	6366	Transcription from Pol II promoter	0.0068	NA	0.0269
Cell proliferation, cell cycle, mitotic checkpoint	8283	Cell proliferation	0.00001	0.003	0.0232
	8151	Cell growth and/or maintenance	0.0041	0.0464	NA
	6275	Regulation of DNA replication	0.0101	0.0101	NA
	278	Mitotic cell cycle	0.0334	0.0084	NA
	79	Regulation of CDK activity	0.0192	NA	NA
	7078	Mitotic metaphase plate congression	0.047	NA	NA
	50790	Regulation of enzyme activity	0.0363	NA	NA
Cell regulation	50789	Regulation of biological process	0.00004	0.00006	0.0016
	50794	Regulation of cellular process	0.0035	0.0007	0.0012
	9987	Cellular process	0.0379	NA	NA

NOTE: The last three columns are the probability that each immediate daughter term (a *P* value) is linked to the number of selected genes by chance; *P* value was calculated using the GO3 software.

Abbreviations: BENDA, bendamustine; CHLB, chlorambucil; NA, no *P* value given: no linkage observed; PM, phosphoramidate mustard (cyclophosphamide metabolite).

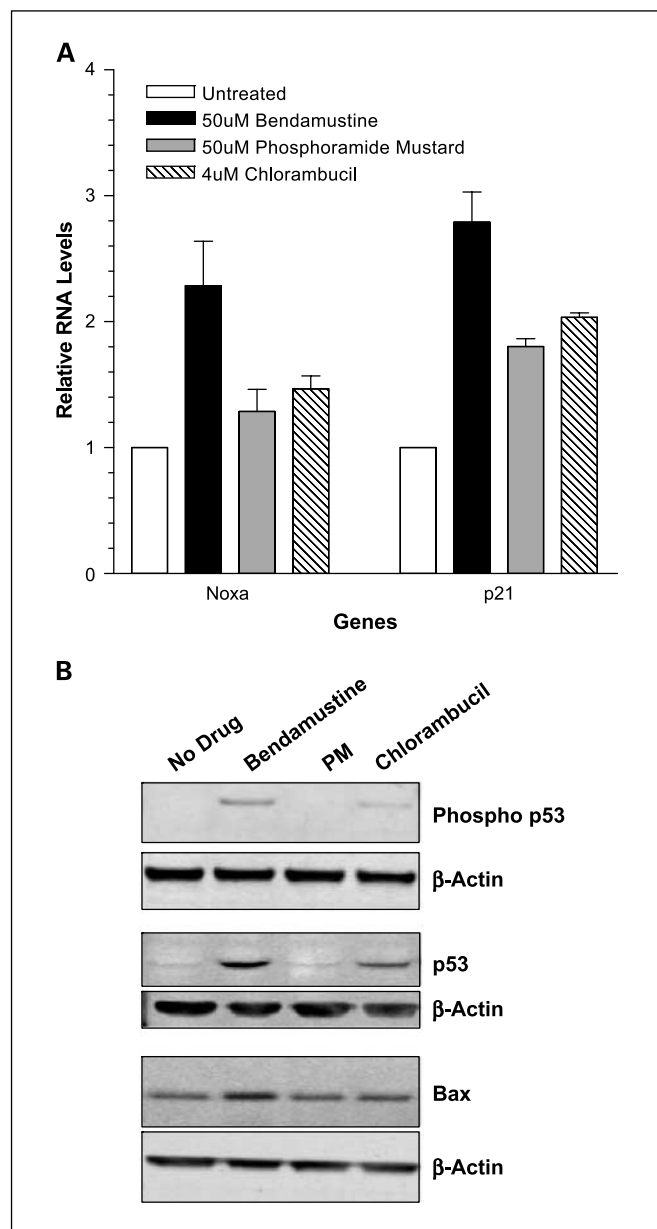


Fig. 2. Enhanced apoptosis signaling by bendamustine when compared with the cyclophosphamide metabolite, phosphoramidate mustard, and chlorambucil. **A**, Q-PCR analysis of SU-DHL-1 cells exposed to equitoxic concentrations of bendamustine, phosphoramidate mustard, and chlorambucil. The levels of input cDNA were normalized using an assay for 18S RNA, and the expression in the untreated sample was set to 1. Columns, mean of the fold changes from DMSO-treated controls; bars, SE. The results were averaged from three independent experiments. **B**, analysis of protein expression of apoptotic regulators was done on SU-DHL-1 cells exposed to bendamustine (50 μ mol/L), phosphoramidate mustard (PM, 20 μ mol/L), and chlorambucil (2 μ mol/L). Cell lysates were prepared after 20-h exposure. β -Actin protein expression served as a loading control and is shown below the regulated proteins. Top, expression of Ser¹⁵-phosphorylated p53, detected using a phosphospecific antibody. Middle, total p53. Bottom, expression of Bax.

activity/resistance profiles observed for bendamustine versus cyclophosphamide and chlorambucil.

To further examine the differences between bendamustine and the other alkylators in DNA damage and induction of DNA repair pathways, we tested the cytotoxic activity of the drugs in the presence of a specific inhibitor of DNA repair. The DNA repair enzyme APE is an apurinic/apyrimidinic endonuclease

that plays a critical role in the base excision repair pathway (33). APE is inhibited by methoxyamine, a drug that specifically binds to abasic sites in DNA and reduces APE activity by >300-fold (34). The cytotoxic activities of bendamustine and phosphoramidate mustard in the presence of methoxyamine were assessed in Raji (a Burkitt's lymphoma cell line) and SU-DHL-1 cells. The IC₅₀ of bendamustine was reduced ~6-fold in the Raji cells and 4-fold with methoxyamine addition. In contrast, the IC₅₀ of phosphoramidate mustard did not change with methoxyamine addition (Fig. 3B). These data indicate that bendamustine uniquely induces a base excision repair pathway response.

The DNA repair enzyme O⁶-alkylguanine-DNA alkyl transferase is an important DNA-repair protein that protects cells from the toxic effects of DNA alkylators. The activity of bendamustine and phosphoramidate mustard was examined in Raji and SU-DHL-1 cell lines in the presence of an alkylguanyl transferase inhibitor, O⁶-benzylguanine. The cytotoxicity of phosphoramidate mustard was increased in both cell lines, whereas that of bendamustine was not enhanced by the addition of O⁶-benzylguanine in either cell line (Fig. 3C). These data indicate that other alkylators but not bendamustine induce an alkyltransferase mechanism of DNA repair.

Bendamustine inhibits mitotic checkpoints and induces mitotic catastrophe. The effect of bendamustine, phosphoramidate mustard, and chlorambucil on cell cycle progression was determined using flow cytometric analysis. SU-DHL-1 cells were treated with equitoxic concentrations of the drugs, or DMSO as a control, for 8 h. Bendamustine caused a significantly greater increase in the proportion of cells in the S-phase of the cell cycle (~60%) compared with chlorambucil (45%) and phosphoramidate (37%), based on the DMSO control (37%; Fig. 4A and B).

One of the most striking results that emerged from the Q-PCR analysis of genes involved in the cell proliferation/cell cycle/mitotic checkpoint molecular functional group identified in the GO analysis was the differential regulation of several mitosis-related genes, including *polo-like kinase 1* (PLK-1), *Aurora Kinase A*, and *cyclin B1*—genes considered very important in mitotic checkpoint regulation (35–40). Treatment with bendamustine resulted in a 60% to 80% down-regulation of the mRNA expression of all three of these genes in SU-DHL-9 cells, whereas phosphoramidate mustard or chlorambucil had more modest inhibitory effects on these gene transcripts (Fig. 4C); the same trend was observed in Daudi cells (a Burkitt's lymphoma cell line; data not shown).

It is possible that a defect in mitotic checkpoints inhibits the "physiologic" arrest of the DNA alkylator-treated cells, required for efficient repair of DNA damage before cells are allowed to enter mitosis. Cells entering mitosis with significant DNA damage are reported to result in activation of the death pathway known as mitotic catastrophe. Mitotic catastrophe is a necrotic form of cell death that occurs during metaphase and is morphologically distinct from apoptosis. It can occur in the absence of functional p53 or in cells where conventional caspase-dependent apoptosis is suppressed (41, 42).

To determine whether bendamustine can cause mitotic catastrophe, it was necessary to find a model in which the apoptotic effects of bendamustine could be distinguished from the potential mitotic catastrophe end point. To this end, bendamustine was tested in cell lines with deficiencies in apoptotic pathways (the multidrug-resistant breast cancer cell line

MCF-7/ADR and a p53-deficient colon cancer cell line, RKO-E6) and in the presence of an inhibitor of classic apoptotic pathways, the pan-caspase inhibitor zVAD-fmk. MCF-7/ADR and RKO-E6 cells were treated for 3 days with 25 $\mu\text{mol/L}$ bendamustine alone or in combination with 20 $\mu\text{mol/L}$ zVAD-fmk. Microscopic analysis of nuclear morphology using 4',6-diamidino-2-phenylindole staining revealed an increased incidence of chromatin condensation and multinucleation/micronucleation, hallmarks of mitotic catastrophe, in both cell lines. Twenty-six percent of the bendamustine-treated MCF-7/ADR cells showed micronucleation compared with only 6% in DMSO control cells (Fig. 4D). Results were similar in RKO-E6 cells (data not shown). These data indicate that in addition to inducing apoptosis, bendamustine may cause mitotic catastrophe.

Discussion

In this report, we describe the characterization of molecular mechanisms of action of bendamustine, in addition to outlining several important differences between bendamustine and other clinically used 2-chloroethylamine DNA-alkylating agents, such as cyclophosphamide and chlorambucil.

Analysis of data from the NCI IVCLSP indicated that other alkylating agents, cyclophosphamide, chlorambucil, and melphalan, have high coefficients of correlation, suggesting that they have very similar mechanistic features. In contrast, a lack of high coefficients of correlation between bendamustine and these drugs suggests that bendamustine exhibits a unique mechanism of action. Results from microarray analyses of bendamustine, the cyclophosphamide metabolite phosphoramidate mustard, and chlorambucil also indicated clear differences between bendamustine and the other alkylating agents, in the form of different trends in gene regulation within distinct functional pathways. Validation of some of the screening results and more detailed cellular assays helped to further

characterize specific molecular mechanisms of action of bendamustine.

Treatment with bendamustine resulted in the initiation of the "canonical" p53-dependent stress pathway that results in a strong activation of intrinsic apoptosis. Bendamustine showed higher levels of p53 activation (phosphorylation at Ser¹⁵) and induction of p53-dependent genes, compared with other alkylating agents. Although other nitrogen mustards have been previously reported to induce a p53-mediated stress response, the data presented here suggest that bendamustine may provide a stronger and more rapidly induced signal compared with equitoxic doses of phosphoramidate or chlorambucil.

Concurrently, bendamustine exposure resulted in inhibition of several mitotic checkpoints. Cells entering mitosis with extensive DNA damage may consequently undergo death by mitotic catastrophe. This alternative cell death pathway, together with the strong activation of apoptosis, may in part explain the effectiveness of bendamustine in drug-resistant cells *in vitro* (11), as well as in lymphoma patients with chemotherapy-refractory disease (1).

Initiation of mitotic catastrophe is an appealing mechanism of tumor cell death because it may also function in tumor cells that have developed resistance to apoptosis following exposure to several rounds using conventional chemotherapeutic drugs. The extensive and durable DNA damage elicited by bendamustine (9) with concomitant inhibition of M-phase-specific checkpoints as well as the observance of multinucleation/micronucleation suggest that mitotic catastrophe is occurring in the treated cells. These latter activities of bendamustine were shown here to be either stronger than other alkylators at equitoxic doses or unique to bendamustine. In addition, bendamustine seems to activate different DNA repair pathways than traditional nitrogen mustards. Cytotoxic activity of bendamustine, but not phosphoramidate, was enhanced by inhibition of the base excision repair DNA damage response pathway, suggesting that bendamustine is more dependent on

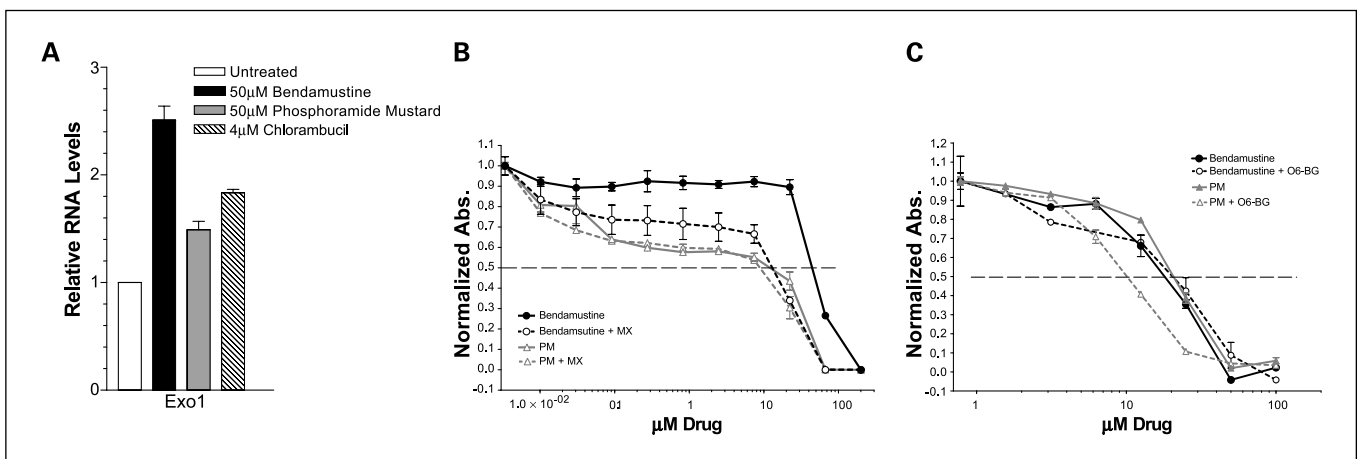


Fig. 3. Bendamustine differentially modifies genes involved in base excision repair. *A*, relative RNA levels of DNA repair enzyme EXO1. Q-PCR analysis was done using SU-DHL-1 cells exposed to equitoxic concentrations of bendamustine, phosphoramidate mustard, and chlorambucil. The levels of input cDNA were normalized using an assay for 18S RNA, and the expression in the untreated sample was set to 1. Columns, mean of the fold changes from DMSO-treated controls; bars, SE. The results were averaged from three independent experiments. *B*, the role of the repair enzyme Ape-1 in the cytotoxic activity of bendamustine and phosphoramidate mustard was assessed using the Ape-1 inhibitor methoxyamine (MX). Cells were preincubated with methoxyamine for 30 min before the drug addition. The IC₅₀ (dashed line) was determined by MTT assay after 72 h incubation with drug. *C*, the role of the repair enzyme O⁶-alkylguanine-DNA alkyl transferase in the cytotoxic activity of bendamustine was assessed using the inhibitor O⁶-benzylguanine (O⁶-BG). The IC₅₀ of bendamustine and phosphoramidate mustard with or without a 30-min preincubation with O⁶-BG was determined by MTT assay after 72 h incubation with drug. The addition of O⁶-benzylguanine did not significantly change the IC₅₀ of bendamustine, although the IC₅₀ of phosphoramidate mustard was reduced 2-fold.

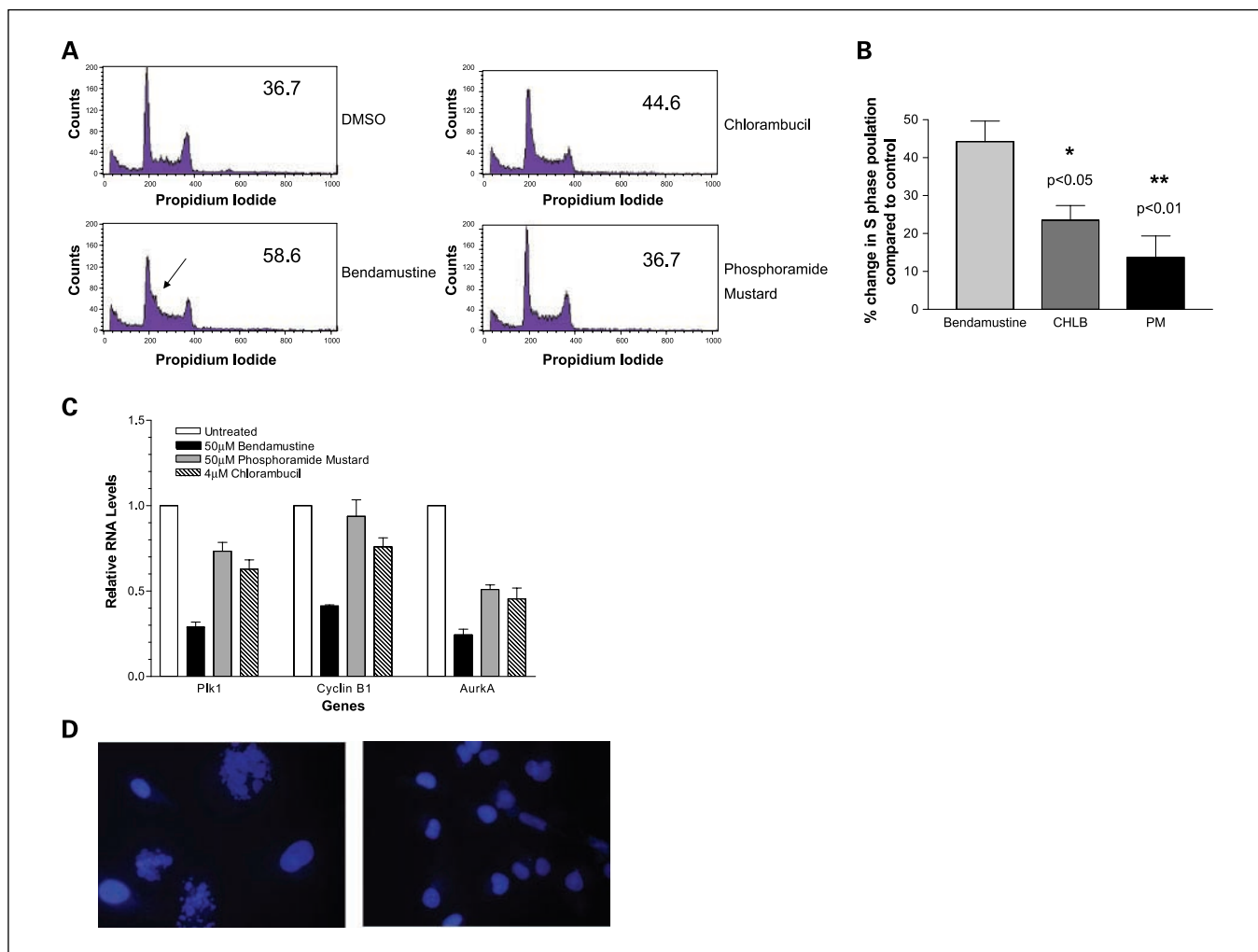


Fig. 4. Bendamustine mediates mitotic catastrophe. *A*, accumulation of cells in S phase: SU-DHL-1 cells were treated with 50 $\mu\text{mol/L}$ bendamustine, 4 $\mu\text{mol/L}$ chlorambucil, 50 $\mu\text{mol/L}$ phosphoramidate mustard (equitoxic concentrations), or diluent DMSO as a control; harvested; and stained for DNA content with propidium iodide. The number in the top right-hand corner of the histogram represents the percentage of the diploid cell population in S-phase as calculated using DNA Modfit LT software (Verity Software House). Arrow, an area of increased cell accumulation in the bendamustine-treated sample. *B*, the change in the percentage of cells in S-phase from the control sample (diluent DMSO). Columns, averaged change from four independent experiments; bars, SD. Statistical significance (*) of the differences between the averaged bendamustine S-phase population distribution and that of chlorambucil (*CHLB*) and phosphoramidate mustard samples were confirmed using the unpaired Student's *t* test. *C*, inhibition of mitotic checkpoints: Q-PCR analysis was done in SU-DHL-1 cells exposed to equitoxic concentrations of bendamustine, phosphoramidate mustard, and chlorambucil. The levels of input cDNA were normalized using an assay for 18S RNA, and the expression in the untreated sample was set to 1. Columns, mean of the fold changes from DMSO-treated controls; bars, SE. The results were averaged from three independent experiments. *D*, mitotic catastrophe: Multidrug-resistant MCF-7/ADR cells were exposed for 3 d to 25 $\mu\text{mol/L}$ bendamustine in the presence of 20 $\mu\text{mol/L}$ of the pan-caspase inhibitor, zVAD-fmk. Microscopic analysis of nuclear morphology using DNA 4',6'-diamidino-2-phenylindole staining revealed an increased incidence of chromatin condensation and micronucleation, hallmarks of mitotic catastrophe, in treated cells (26%; left) compared with untreated cells (6%; right). Extensive cell death was observed in the treated population of cells.

this response. In contrast, the addition of an alkyltransferase inhibitor (*O*⁶-benzylguanine) potentiated phosphoramidate cytotoxicity but had no effect on the activity of bendamustine. These data suggest that bendamustine does not induce an alkyltransferase mechanism of DNA repair. Past studies have also documented increased cytotoxicity of melphalan and chlorambucil, in addition to phosphoramidate, in the presence of *O*⁶-benzylguanine (43). These data suggest that bendamustine may be less susceptible to drug resistance based on alkylguanyl transferase expression.

These mechanistic differences may offer potential explanations for the efficacy of bendamustine in patients with relapsed disease, which is refractory to other alkylating agents. The differences described here, as well as the activity of bendamustine

in patients refractory to chemotherapy, support further study of bendamustine combined with other alkylating agents. Consequently, bendamustine represents an important addition to the armamentarium of the clinician for the treatment of patients with relapsed, refractory indolent non-Hodgkin's lymphoma and potentially many other cancers.

Acknowledgments

We thank the Developmental Therapeutics Department of the NCI/NIH for testing bendamustine in their anticancer screening program and for supplying phosphoramidate mustard cyclohexylamine salt, Dr. Charlie Rodi for helpful suggestions and discussion, and Bridget O'Keefe, Ph.D., for writing support.

References

- Friedberg JW, Cohen P, Chen L, et al. Bendamustine in patients with rituximab-refractory indolent and transformed non-Hodgkin's lymphoma: results from a phase II multicenter, single-agent study. *J Clin Oncol*. In press 2007.
- Rummel MJ. Bendamustine plus rituximab is effective and has a favorable toxicity profile in the treatment of mantle cell and low-grade non-Hodgkin's lymphoma. *J Clin Oncol* 2005;23:3383–9.
- Bergmann MA. Efficacy of bendamustine in patients with relapsed or refractory chronic lymphocytic leukemia: results of a phase I/II study of the German CLL Study Group. *Haematologica* 2006;90:1357–64.
- Knop S, Straka C, Haen M, Schwedes R, Hebart H, Einsele H. The efficacy and toxicity of bendamustine in recurrent multiple myeloma after high-dose chemotherapy. *Haematologica* 2005;90:1287–8.
- Ponisch W, Mitrou PS, Merkle K, et al. Treatment of bendamustine and prednisone in patients with newly diagnosed multiple myeloma results in superior complete response rate, prolonged time to treatment failure and improved quality of life compared to treatment with melphalan and prednisone—a randomized phase III study of the East German Study Group of Hematology and Oncology (OSHO). *J Cancer Res Clin Oncol* 2006;132:205–12.
- von Minckwitz G, Chernozemsky I, Sirakova L, et al. Bendamustine prolongs progression-free survival in metastatic breast cancer (MBC): a phase III prospective, randomized, multicenter trial of bendamustine hydrochloride, methotrexate and 5-fluorouracil (BMF) versus cyclophosphamide, methotrexate and 5-fluorouracil (CMF) as first-line treatment of MBC. *Anticancer Drugs* 2005;16:871–7.
- Schmittel A. Phase II trial of second-line bendamustine chemotherapy in relapsed small cell lung cancer patients. *Lung Cancer* 2007;55:109–13.
- Koster W. Phase II trial with carboplatin and bendamustine in patients with extensive stage small-cell lung cancer. *J Thoracic Oncol* 2007;2:312–16.
- Strumberg D, Harstrick A, Doll K, Hoffmann B, Seeber S. Bendamustine hydrochloride activity against doxorubicin-resistant human breast carcinoma cell lines. *Anticancer Drugs* 1996;7:415–21.
- Wosikowski K. The effect of bendamustine is slightly decreased by P-glycoprotein and MXR/BCRP resistance mechanism. Munich: Klinge Pharma Fujisawa Group; 2000. Report No. 0640.00.C07.02 1–14.
- Leoni LM, Niemeyer CC, Kerfoot C, et al. *In vitro* and *ex vivo* activity of SDX-105 (bendamustine) in drug-resistant lymphoma cells [abstract 1215]. *Proc Am Assoc Cancer Res* 2004;45:278.
- Bremer K. High rates of long-lasting remissions after 5-day bendamustine chemotherapy cycles in pretreated low-grade non-Hodgkin's lymphomas. *J Cancer Res Clin Oncol* 2002;128:603–9.
- Ozegowski W, Krebs D. IMET 3393, (-[1-methyl-5-bis-(chloroethyl)-amino-benzimidazolyl-(2)]-butyric) acid hydrochloride, a new cytostatic agent from among the series of benzimidazole mustard compounds. *Zbl Pharm* 1971;110:1013–9.
- Woolley DW. Some biological effects produced by benzimidazole and their reversal by purines. *J Biol Chem* 1944;152:225–32.
- Hirschberg E, Gellhorn A, Gump WS. Laboratory evaluation of a new nitrogen mustard, 2-[di-(2-chloroethyl) aminomethyl] benzimidazole and of other 2-chloroethyl compounds. *Cancer Res* 1957;17:904–10.
- Hartmann M, Zimmer C. Investigation of cross-link formation in DNA by the alkylating cytostatic IMET 3106, 3393 and 3943. *Biochim Biophys Acta* 1972;287:386–9.
- Zong WX, Ditsworth D, Bauer DE, Wang ZQ, Thompson CB. Alkylating DNA damage stimulates a regulated form of necrotic cell death. *Genes Dev* 2004;18:1272–82.
- Nowak D, Boehrer S, Brieger A, et al. Upon drug-induced apoptosis in lymphoma cells X-linked inhibitor of apoptosis (XIAP) translocates from the cytosol to the nucleus. *Leuk Lymphoma* 2004;45:1429–36.
- Konstantinov SM, Kostovski A, Topashka-Ancheva M, Genova M, Berger MR. Cytotoxic efficacy of bendamustine in human leukemia and breast cancer cell lines. *J Cancer Res Clin Oncol* 2002;128:271–8.
- Schwanen C, Hecker T, Hubinger G, et al. *In vitro* evaluation of bendamustine induced apoptosis in B-chronic lymphocytic leukemia. *Leukemia* 2002;16:2096–105.
- Chow KU, Nowak D, Boehrer S, et al. Synergistic effects of chemotherapeutic drugs in lymphoma cells are associated with down-regulation of inhibitor of apoptosis proteins (IAPs), prostate-apoptosis-response-gene 4 (Par-4), death-associated protein (Daxx) and with enforced caspase activation. *Biochem Pharmacol* 2003;66:711–24.
- Monks A, Scudiero D, Skehan P, et al. Feasibility of a high-flux anticancer screen using a diverse panel of cultured human tumor lines. *J Natl Cancer Inst* 1991;83:757–66.
- Paull KD, Shoemaker RH, Hodes L, et al. Display and analysis of patterns of differential activity of drugs against human tumor cell lines: development of mean graph and COMPARE algorithm. *J Natl Cancer Inst* 1989;81:1088–92.
- Paull KD, Hamel E, Malspeis L. Prediction of biochemical mechanism of action from the *in vitro* antitumor screen of the National Cancer Institute. In: Foye WO, editor. *Cancer chemotherapeutic agents*. Washington (DC): American Chemical Society; 1995. p. 9–45.
- Ludeman SM. The chemistry of the metabolites of cyclophosphamide. *Curr Pharm Des* 1999;5:627–43.
- Kufe D, Pollock R, Weichselbaum R, et al, editors. *Holland-Frei cancer medicine* 6. London: BC Decker; 2003.
- Sasik R, Calvo E, Corbeil J. Statistical analysis of high-density oligonucleotide arrays: a multiplicative noise model. *Bioinformatics* 2002;18:1633–40.
- Livak KJ, Schmittgen TD. Analysis of relative gene expression data using real-time quantitative PCR and the 2(- $\Delta\Delta C(T)$) method. *Methods* 2001;25:402–8.
- Leoni LM, Hamel E, Genini D, et al. Indanocine, a microtubule-binding indanone and a selective inducer of apoptosis in multidrug-resistant cancer cells. *J Natl Cancer Inst* 2000;92:217–24.
- Houghton JA. Apoptosis and drug response. *Curr Opin Oncol* 1999;11:475–81.
- Secchiero P, Vaccarezza M, Gonelli A, Zauli G. TNF-related apoptosis-inducing ligand (TRAIL): a potential candidate for combined treatment of hematological malignancies. *Curr Pharm Des* 2004;10:3673–81.
- De Feudis P, Vignati S, Rossi C, et al. Driving p53 response to Bax activation greatly enhances sensitivity to Taxol by inducing massive apoptosis. *Neoplasia* 2000;2:202–7.
- Evans AR, Limp-Foster M, Kelley MR. Going APE over ref-1. *Mutat Res* 2000;461:83–108.
- Horton JK, Prasad R, Hou E, Wilson SH. Protection against methylation-induced cytotoxicity by DNA polymerase β -dependent long patch base excision repair. *J Biol Chem* 2000;275:2211–8.
- Blagden S, de Bono J. Drugging cell cycle kinases in cancer therapy. *Curr Drug Targets* 2005;6:325–35.
- Liu X, Erikson RL. Polo-like kinase 1 in the life and death of cancer cells. *Cell Cycle* 2003;2:424–5.
- Marumoto T, Honda S, Hara T, et al. Aurora-A kinase maintains the fidelity of early and late mitotic events in HeLa cells. *J Biol Chem* 2003;278:51786–95.
- Scaife RM. G2 cell cycle arrest, down-regulation of cyclin B, and induction of mitotic catastrophe by the flavoprotein inhibitor diphenyleneiodonium. *Mol Cancer Ther* 2004;3:1229–37.
- Hauf S, Cole RW, LaFerrà S, et al. The small molecule Hesperadin reveals a role for Aurora B in correcting kinetochore-microtubule attachment and in maintaining the spindle assembly checkpoint. *J Cell Biol* 2003;161:281–94.
- Cogswell JP, Brown CE, Bisi JE, Neill SD. Dominant-negative polo-like kinase 1 induces mitotic catastrophe independent of cdc25C function. *Cell Growth Differ* 2000;11:615–23.
- Castedo M, Perfettini JL, Roumier T, Andreau K, Medema R, Kroemer G. Cell death by mitotic catastrophe: a molecular definition. *Oncogene* 2004;23:2825–37.
- Castedo M, Perfettini JL, Roumier T, et al. Mitotic catastrophe constitutes a special case of apoptosis whose suppression entails aneuploidy. *Oncogene* 2004;23:4362–70.
- Cai Y, Ludeman SM, Wilson LR, Chung AB, Dolan ME. Effect of *O*⁶-benzylguanine on nitrogen mustard-induced toxicity, apoptosis, and mutagenicity in Chinese hamster ovary cells. *Mol Cancer Ther* 2001;1:21–8.